IEE Conference Publication Number 216

RADAR 1982

International Conference

RADAR-82

18—20 October 1982

Organised by the
Electronics Division of the Institution of Electrical Engineers

in association with the
Institute of Electrical and Electronics Engineers
(Aerospace and Electronic Systems Society)

with the support of the
Convention of National Societies of
Electrical Engineers of Western Europe (EUREL)
Institute of Mathematics and its Applications
Institution of Electronic and Radio Engineers
Royal Aeronautical Society
Royal Institute of Navigation

Venue
The Royal Borough of Kensington and Chelsea Town Hall,
Hornton Street, London W8, UK

Organising Committee

K F Slater (*Chairman*)
P K Blair
Dr J Clarke
Professor J R Forrest
K L Fuller
R N Lord*
Dr K Milne OBE
M F Radford
M H A Smith
F K Spokes
C M Stewart
P D L Williams

Overseas Corresponding Members

Colonel E Arkoumaneas, Greece
E P W Attema, Netherlands
Professor M H Carpentier, France
Dr A L Gilardini, Italy
Professor P Gudmandsen, Denmark
R T Hill, USA**
Professor G F Lind, Sweden
Dr T Lund, Norway
Professor S Okamura, Japan
Dr W D Wirth, Federal Republic of Germany

**representing the Institute of Electrical and Electronics Engineers (Aerospace and Electronic Systems Society)
*representing the Institution of Electronic and Radio Engineers

The cover design is a reproduction of a radar display of the Spithead Review of the Fleet on the occasion of Her Majesty The Queen's Silver Jubilee in 1977.

The radar display is reproduced by permission of the Ministry of Defence (PE) at the Admiralty Surface Weapons Establishment, Portsdown. Crown copyright reserved.

Published by the Institution of Electrical Engineers, London and New York, ISBN 0 85296268 1 ISSN 0537-9989.

Produced by MULTIPLEX techniques ltd, Orpington, Kent.

Contents

The Institution of Electrical Engineers is not, as a body, responsible for the opinions expressed by individual authors or speakers.

Contents

* *The text of this contribution was not available at the time of publication.*

Contents

Contents

Contents

Contents

Contents

Contents

List of Authors

List of Authors

ADAPTIVE RADAR IN REMOTE SENSING USING SPACE, FREQUENCY AND POLARIZATION PROCESSING

Dag T. Gjessing and Jens Hjelmstad

Royal Norwegian Council for Scientific and Industrial Research, Environmental Surveillance Technology Programme

1 INTRODUCTION

The radar scientist is facing a challenging and inspiring future, one of matching new technological achievements to important applications in the field of remote detection and identification.

This contribution is dedicated to the following concept: Most of the existing detection/identification systems do not make optimum use of all the a priori information on the object of interest that one generally is in possession of. Knowing something about the geometrical shape of the object on which our attention is focused (distribution of scattering centers and motion pattern), an optimum illumination and detection system which adapts itself to this target against a terrestrial background through an adverse propagation medium can be designed.

We are thus faced with the consideration of three filter functions: the transmission medium between the observation platform and the target, the terrestrial background against which the target is viewed, and the target itself. The more detailed information we require about the particular target per unit time, the more widebanded must our radar illuminator be.

In this brief contribution we shall concentrate on the multifrequency radar system. As we shall see, this system lends itself directly to simple computer control in a manner which is very familiar to the computer scientist.

Having structured the illumination in the time domain for optimum coupling to the target, it remains to shape the phasefront in space so as to obtain maximum coupling to the particular reflecting structure of interest by making use of a matrix antenna (two-dimensional broadside array).

Finally, we can manipulate the polarization properties of our transmit/receive system so as to investigate the polarization characteristics (the symmetry properties) of the target.

In this brief presentation we shall lean heavily on earlier contributions from the authors' laboratory (1,2,3,4,5), highlight these and describe a multi-frequency polarimetric radar system which presently is being developed by the authors. We shall present results from simple mathematical models and offer some preliminary experimental verifications.

2 BASIC PHYSICAL CONCEPTS: FORMULATION OF THE PROBLEM

As introduced above, we shall be considering four signature domains:

a) By measuring the correlation properties $R(\Delta F)$ in the frequency domain of the waves scattered back from the illuminated area (target against background) we obtain information about the longitudinal distribution of the scatterers. Specifically it can be shown (1,2,3,4,5) that if we describe the distribution in range (longitudinally) of the scatterers by the delay function $f(z)$ which has dimension field-strength and is the square root of the scattering cross-section $\sigma(z)$, then the correlation function in the frequency domain $R(\Delta F)$ is the Fourier transform of $f(z)$. A measure of $R(\Delta F)$ is obtained, as we know, by multiplying the scattered field-strength of frequency F by the complex conjugate of the field-strength at frequency $F+\Delta F$.

Thus we have

$$E(F)\ E^*(F+\Delta F) \sim R(\Delta F)$$

$$\sim FT\{R(\Delta z)\} \qquad (2.1)$$

Note that if the target is illuminated with two frequencies spaced ΔF apart, then irregularities in the target with scale size $\Delta z = c/(2\Delta F)$ contribute to the scattered field.

b) By measuring the spatial correlation properties of the field scattered back from the target in a plane normal to the direction of propagation, i.e. transversely, we obtain information about the transverse distribution of the scatterers. If then the x and y directions are orthogonal to the direction of propagation z (direction from radar to target), then we measure the field-strength at the points x and $x+\Delta x$ in exactly the same way as above where we were dealing with different frequencies.

It can here readily be shown (page 18 of reference 2) that

$$E(x)\ E^*(x+\Delta x) \sim R(\Delta x)$$

$$\sim FT\{\sigma(x/R)\} \qquad (2.2)$$

where $\sigma(x)$ is the transverse distribution of the scatterers over the scattering body in the x direction and R is the distance to the target. This, of course, is the same as saying that the spatial auto-correlation of the transverse field-strength is the Fourier transform of the angular power spectrum of the scattered wave (angle of arrival spectrum).

c) By measuring the temporal distribution of the scattered field (the power spectrum) information about the motion pattern of the target is obtained through the well-known Doppler relationship

$$f = \frac{1}{2\pi}\ \vec{k}\cdot\vec{V} \qquad (2.3)$$

where f is the Doppler frequency, $\vec{K}$ is the vector difference $\vec{k}_i-\vec{k}_s$ between the wavenumber $\vec{k}_i$ of the illuminating (incident) wave and $\vec{k}_s$ the wavenumber of the scattered wave. $\vec{V}$ is the velocity of the scattering element.

Thus if we are dealing with a target (such as the sea surface) composed of many scattering centers or facets which have different velocity, we obtain information about the velocity distribution of scale size Δz by illuminating the target with two frequencies with frequency difference $\Delta F = c/(2\Delta z)$ and by measuring the temporal variation (power spectrum) of the quantity

$$W(\omega) \sim V(F,t)\, V^*(F+\Delta F,t) \qquad (2.4)$$

Note that the velocity of the scattering element of scale size Δz is obtained from equation (2.3) by noting that it is the wavenumber $\Delta K = 2\pi/\Delta z$ of the difference frequency ΔF that enters into the Doppler equation in this case.

Hence the Doppler frequency is given by

$$f = \frac{2\Delta F}{c} \cos \phi$$

For details the reader is referred to ref (5), page 15.

d) By measuring the distribution of the scattering centers (the $\sigma(z)$, $\sigma(x)$ and $\sigma(y)$ functions) for each element of the scattering matrix, we obtain information about the symmetry characteristics of the target.

Figure 2.1 finally sums up the basic concepts of the general adaptive (inverse scattering) radar system, whereas figure 2.2 shows the radar signature (correlation function in the frequency domain) of some idealized scattering objects. Note that the spatial correlation function is obtained by changing the abscissa of figure 2.2 from ΔF to $R\lambda/\Delta x$.

Before we proceed to give experimental verifications of the simple mathematical models based on first principle physics, let us consider the basics of polarimetry in relation to a multi-frequency radar system. Single frequency pulsed polarimetric radars have recently received considerable attention (6-9); in this very space limited presentation, we shall confine ourselves to introducing the basic concepts involved in an experimental investigation which is in progress at the authors' laboratory aiming at increasing the target identification potential of our multi-frequency radar system. Note that the present radar (see figure 3.1) makes use of six correlated computer controlled frequency synthesizers which will give 15 different frequency spacings (can couple to 15 different target scales). The radar has two transmitters and two receivers with polarization control so as to enable us to determine the frequency covariance function

$$R(\Delta F) \sim V(F)\, V^*(F+\Delta F)$$

simultaneously for 15 frequency separations and for the three polarization combinations (horizontal/horizontal (S_{11}), horizontal/vertical (S_{12})and vertical/vertical (S_{22}). The radar can also operate with adaptive polarization basis, that is, the radar optimizes its detection and identification capability by transmitting the optimal elliptic polarization.

After having completed the preliminary tests with this system, the program will be expanded so as to include six spaced receivers so as to allow us to determine the spatial correlation properties of scattered field with 15 spatial separations.

In order to introduce this concept, figure 2.3 is presented. Here we have "modelled" a target in the form of an airplane making use of seven isotropic and polarization invariant scattering centers. Note that the scattering matrix elements merely are represented by their moduli. The actual system, however, measures their relative phase thus allowing detailed analysis of the target's symmetry properties within each time/space resolution in an arbitrary polarization basis.

Figure 2.3 refers to the longitudinal case where the target is viewed head on with 15 coherent frequency spacings. The idealized delay function is shown and the corresponding frequency covariance function $R(\Delta F)$.

In exactly the same way, the spatial correlation of the scattered field can be calculated, giving a $R\lambda/\Delta x$ abscissa rather than a ΔF abscissa.

Having introduced the multi-domain adaptive radar designed primarily for environmental surveillance applications, we shall present a somewhat more general target configuration and give the $R(\Delta F)$ signatures for the three pertinent polarization configurations.

Figure 2.4 shows the simplified air plane target viewed head on with our 15 frequency spacings and three polarization combinations. Note that as in figure 2.3 the target has seven scattering centers. However, as a means of illustrating the polarization issue, we have selected four different classes of scattering in figure 2.4 with the following notations:

-- scatterers for horizontal/horizontal S_{11}
| scatterers for vertical/vertical S_{22}
| odd-bounce scatterers
< even-bounce scatterers

Note that to the extent that the target has polarization sensitive scattering centers, we can draw conclusions regarding detailed aircraft dimensions, not merely overall length as in the case of the simplest scheme illustrated in figure 2.2.

3 A BRIEF DESCRIPTION OF THE RADAR SYSTEM

The adaptive polarimetric multi-frequency radar system shown in figure 3.1 is made from a conventional 960 channel microwave communications link. The system structure is, as indicated in the figure, very simple. The six frequencies in the 50 - 90 MHz band delivered from a common crystal oscillator are up-converted to the 6 GHz band giving a total output power of 200 mW (33 mW per frequency) to the transmitting antenna. Two different antennas were used for the various applications: a horn antenna with an aperture of 30 x 30 cm and a paraboloid with diameter 1.20 m.

The receiving antenna was positioned adjacent to the transmitter (110 dB isolation). Transmitting and receiving antennas are identical. The backscattered signal is down-converted to the IF band (50 - 90 MHz) by means of a 6 GHz source. This source is xtal-controlled and common to both the up- and down convertors. Upon amplification and filtering, the six separate VHF receiver frequencies are mixed with the corresponding six frequencies from the transmitting synthesizers. The resulting 6 voltages giving 15 different frequency pairs are then multiplied and the products (the 15 covariances $V(F,t)\ V^*(F+\Delta F,t)$ resulting) are subjected to 15 sets of Fast Fourier Transform filters, thus producing 15 power spectra (Doppler spectra).

The essence of these processes is illustrated in figure 4.1.

4 EXPERIMENTAL VERIFICATIONS

The multi-frequency radar system was used for three different investigations:

- Measurement of directional ocean wave spectra (wave intensity, velocity and direction)
- Investigation of ship signatures against a sea background
- Classification of air targets (F-16 aircraft)

A brief highlighting of the results of these investigations will now be given.

4.1 Directional ocean wave spectra

Illuminating the sea surface from a cliff 50 m above the sea, the ocean wave spectra (wave intensity and wave velocity) was determined for various azimuth directions and for 15 different ocean wavelengths in the interval from some 5 m (couples to ΔF = 27 MHz) to 150 m (corresponding to ΔF = 1 MHz). For each frequency separation ΔF the power spectrumn of the frequency covariance function $V(F,t)\ V^*(F+\Delta F,t)$ was computed.

Examples of such power spectra (Doppler spectra) are shown in the upper part of figure 4.1. In the lower part of the figure two curves are plotted: The curve marked with crosses gives the wave intensity (wave height) spectrum for ocean wavelengths ranging from 18 to 150 m. The curve marked with points gives the Doppler shift as a function of ocean wavelength obtained from the power spectra shown in the upper part of the figure. Note that the theoretical Doppler shift (phase velocity of gravity waves given by:

$$V = \sqrt{\frac{gL}{2\pi}}$$ where L is the ocean wavelength

(ref 4)) is also shown. The systematic shift of the experimental points towards higher velocity is probably due to tidal currents on which the wave motion is superimposed. We obtain one such set of spectra for each azimuth direction of the antenna system.

4.2 Radar signature of a ship against a sea clutter background

Let us focus our attention on ship targets obtained experimentally. Figure 4.2 shows the time-record of the frequency covariance function $V(F,t)\ V^*(F+\Delta F,t)$. To illustrate the essential features, three values of ΔF (out of the total ensemble of 15 frequencies) have been selected. We see that when the radar beam illuminates the sea surface only, the time-record shows an irregular structure. When the ship enters the radar beam, a Doppler signature which is proportional to the frequency separation ΔF is clearly shown.

Before we change the subject from sea surface targets to aircraft, let us present another two sets of experimental results on ship signatures against a sea clutter background. With reference to figure 4.2 above, figure 4.3 shows the Doppler shift for the various frequency separations caused by the ship and by the sea surface, respectively. Note that the ship gives a linear (non-dispersive) relationship between frequency separation and Doppler shift whereas the sea surface gives results which are in reasonably good agreement with the theoretical relationship for deep water gravity waves.

Finally, figure 4.4 shows the normalized correlation as a function of frequency separation for a particular cargoship and also for the sea surface background. Note that the sea surface signature is expanded by a factor 10^3 relative to the signature of the ship. Note also that there is a remarkably good agreement between experimental results and the theoretical ones if the assumption is made that the scatterers are distributed evenly over the scattering body 37.5 m long.

4.3 Radar signature of a rigid airplane

Finally, we shall present a very brief highlightening of the radar signature investigations which were carried out for various types of air targets. In this brief presentation we shall focus our attention on a particular rigid aircraft, namely the F-16 fighter airplane. Tests were also performed on airplanes of comparable size, but different structure. These produced drastically different signatures both as regards the Doppler spectrum (flutter and vibrations superimposed on a translatory motion) and as regards the frequency covariance function. Figure 4.5 shows the signature for the F-16 airplane. Note that by-and-large the agreement with theory when the assumption is made that the scatterers are distributed in a Gaussian manner is reasonably good. There is clear evidence, however, of a small number of scattering centers which dominate over the Gaussian distribution. For details the reader is referred to ref (3).

5 ACKNOWLEDGEMENT

The authors would like to acknowledge the very valuable services rendered by Dr Dagfin Brodtkorb of A/S Informasjonskontroll who laboriously and conscientiously developed the computer software and played a very active role in the planning of the data analysis.

The multi-frequency radar is based on a 960 channel radio relay link generously provided by Mr Standahl of A/S Elektrisk Bureau, Division NERA.

Chief Scientist Karl Holberg of the Norwegian Defence Research Establishment, the previous affiliation of the authors, has been a continuous source of stimulation and encouragement, and we are also indebted to Mr Per Ersdal of the Norwegian Defence Communication Administration who provided antennas and test facilities.

REFERENCES

1. Gjessing, D.T., 1978, "Remote surveillance by electromagnetic waves for air-water-land", Ann Arbor Publishers Inc., Ann Arbor, USA.

2. Gjessing, D.T., 1981, "Adaptive radar in remote sensing", Ann Arbor Publishers Inc., Ann Arbor, USA.

3. Gjessing, D.T., Hjelmstad, J., Lund, T., 1982, "A multifrequency adaptive radar for detection and identification of objects. Results on preliminary experiments on aircraft against a sea clutter background", IEEE Trans., AP-30, 3, 351-365.

4. Gjessing, D.T., Hjelmstad, J., Lund, T., "Directional ocean spectra as observed with a Multi-Frequency CW Doppler Radar System", Submitted for publication.

5. Gjessing, D.T., 1981, "Adaptive techniques for radar detection and identification of objects in an ocean environment", IEEE Journal of Ocean Engineering, OE-6.1, 5-17.

6. Boerner, W.-M., Chan, C.-Y., Mastoris,P., El-Arini, M.B., 1981, "Polarization dependence in electromagnetic inverse problems", IEEE Transactions on Antennas and Prop., AP-29.

7. Huynen, J.R., 1970, "Phenomenological theory of radar targets", PhD Dissertation, Drukherij Bronder-Offset, N.V. Rotterdam.

8. Poelmann, A.J., 1979, "Reconsideration of the target detection criterion based on adaptive antenna polarization", Tijdschrift van het Nederlands Electronica en Radiogenootschap, 44.

9. Deschamps, G.A., 1951, "Geometrical representation of the polarization of a plane electromagnetic wave", Proc. IRE, 39.

10. Bass, F.B., Fuks, I.M., 1979, "Wave scattering from statistically rough surfaces, Pergamon, New York.

11. Plant, W.J., 1977, "Studies of backscattered sea return with a CW dual-frequency X-band radar", IEEE Trans. Antennas and Propagation, AP-25, 1, 28-36.

12. Weissmann, D.E., Johnson, J.W., 1977, "Dual frequency correlation radar measurements of the height statistics of ocean waves", IEEE Journal of Oceanic Eng. OE-77, 74-83.

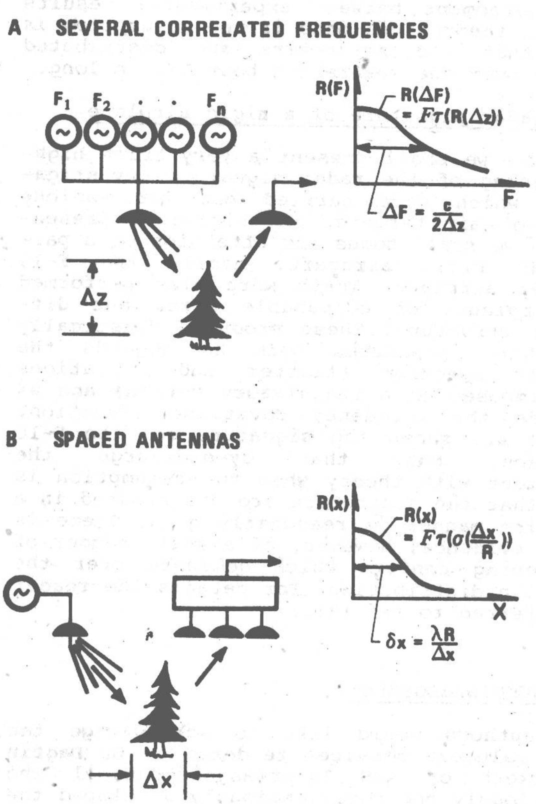

Figure 2.1 The basic concepts of the general adaptive (inverse scattering) radar system

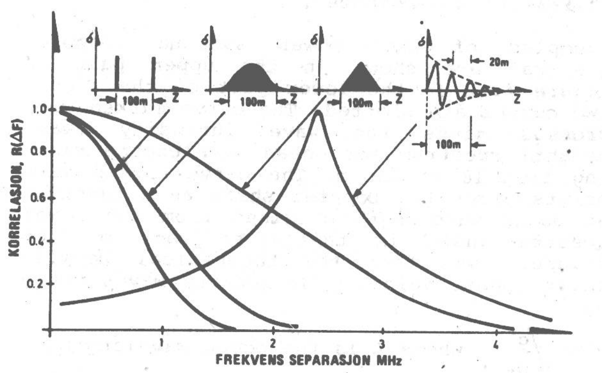

Figure 2.2 The radar signature (correlation function) of some simple scattering objects